

# DYNAMICS OF AN AIRCRAFT IN TURBULENT ATMOSPHERE

M.A. Katary  
Airforce R&D Center,  
Cairo, Egypt.

## ABSTRACT

The present work investigates the airplane dynamics when flying in turbulent atmosphere. Particular attention has been devoted to the evaluation of an RPV longitudinal motion response characteristics at such conditions. A description of the kinematics of turbulent air motion is systematized, and its analytical model is established on the basis of Dryden model. The analysis is performed in both frequency and time domains which allowed a qualitative and quantitative representation of the effects of different parameters. The study demonstrates the importance of flight altitude effect on the RPV resistibility to turbulent air. Besides, both of the flight speed and static stability showed a favorable effect on the airplane dynamic behavior at these circumstances. Finally, the study indicates the prevailing necessity of weather forecast to avoid flight in thunderstorm turbulent air conditions.

*Keywords: Airplane dynamics, Turbulent atmosphere, Response characteristics, Longitudinal motion, Thunderstorm turbulence, Altitude corrector.*

## Nomenclature

b	Wing span, m.	W	Downward velocity, $\text{ms}^{-1}$ .
g	Gravity acceleration, $\text{m.s}^{-2}$ .	w	Perturbed downward velocity, $\text{ms}^{-1}$ .
$I_{YY}$	Moment of inertia, $\text{kgm}^2$ .	$X_{Tu}$	Variation of thrust and X-force with speed, $\text{Nsm}^{-1}$ .
L	Lift force, N.	$X_{T\alpha}$	Variation of thrust and X-force with angle of attack, N.
M	Pitching moment, Nm.	$X_{\delta_e}$	Variation of X-force with elevator angle, N.
m	Mass of airplane, kg.	$Z_q$	Dimensional variation of Z-force with pitch rate, Ns.
$M_u$	Variation of pitching moment with speed, Ns.	$Z_u$	Variation of Z-force with speed, $\text{Nsm}^{-1}$ .
$M_q$	Variation of pitching moment with pitch rate, Nms.	$Z_\alpha$	Variation of Z-force with angle of attack, N.
$M_\alpha$	Variation of pitching moment with angle of attack, Nm.	$Z_\dot{\alpha}$	Variation of Z-force with rate of change of angle of attack, Ns.
$M_\dot{\alpha}$	Variation of pitching moment with rate of change of angle of attack, Nm.	$Z_{\delta_e}$	Variation of Z-force with elevator angle, N.
$M_{\delta_e}$	Variation of pitching moment with elevator angle, Nm.	$\alpha$	Angle of attack.
q	Perturbed pitch rate, $\text{s}^{-1}$ .	$\alpha_g$	Variation of angle of attack due to gust.
$q_g$	Variation of pitch rate due to gust, $\text{s}^{-1}$ .	$\alpha_\delta$	Angle of attack effectiveness of a control surface.
S	Surface area, Reference wing area, $\text{m}^2$ .	$\delta_e$	Elevator angle.
s	Laplace variable.	$\zeta$	Input signal (excitation).
T	Thrust, N.	$\theta$	Pitch attitude angle (perturbed).
U	Forwarded velocity, $\text{ms}^{-1}$ .	$\lambda$	Wave length, m.
u	Perturbed forwarded velocity, $\text{ms}^{-1}$ .	$\Phi_{ug}$	Spectrum function of horizontal wind component.
$u_g$	Horizontal wind component, $\text{ms}^{-1}$ .		
$w_g$	Vertical wind component, $\text{ms}^{-1}$ .		

- $\Phi_{wg}$  Spectrum function of vertical wind component.
- $\Omega$  Spatial frequency,  $s^{-1}$ .
- $\omega$  Frequency,  $s^{-1}$ .

configuration on the response characteristics are evaluated and analyzed.

MATHEMATICAL MODEL:

INTRODUCTION

One of those obstacles with which nature faces man in his use of the air as a medium of transportation, is the turbulent movement of the surrounding air that disturbs his vehicle and its flight path. The wind and wind gusts created by the movement of atmospheric air masses can degrade the performance and flying qualities of an airplane. Besides, wind shears created by thunderstorm turbulence have been identified as the major contributor to several airplanes crashes [1].

For remotely piloted vehicles, this phenomenon gains a special importance since it affects the utilization capability of the RPV as a reconnaissance means. Accordingly, this work proceeds from, and updates, earlier investigations on airplane dynamics when flying in turbulent atmosphere.

It is conventional to consider the effect of wind velocity on airplane flight in the form of a sum of two components, one is constant, and the other is variable. While the first component is of fixed magnitude and direction (deterministic), the second one is variable (behaves as a stationary random variable). Only the latter one is considered in this work as it characterizes the turbulence in atmosphere.

The dynamic equations of the airplane longitudinal motion are derived. The effect of turbulent air is introduced in the aerodynamic components for the cases with and without auto pilot. The mathematical model of the air turbulence components are determined on the basis of Dryden model [4]. Consequently, the airplane transfer functions are obtained for different wind velocity components.

Whereas, in most of recent works, analysis is limited to the frequency domain, in the present work analysis in both frequency and time domains is achieved. The filter technique is used to rearrange the airplane transfer functions to be solved in the time domain using a digital analysis technique. Finally, the influences of flight conditions, turbulence types and parameters, and RPV

The dynamic equations of longitudinal motion for a rigid airplane w.r.t. the principle coordinate system are given as [1] :

$$\dot{u} = -g \cdot \cos \theta_1 \theta + (X_u + X_{Tu}) u + X_\alpha \alpha + X_{\delta e} \delta e$$

$$\dot{w} = -g \cdot \sin \theta_1 \theta + Z_u u + Z_\alpha \alpha + Z_{\dot{\alpha}} \dot{\alpha} +$$

$$(U_1 + Z_q) q + Z_{\delta e} \delta e$$

$$\dot{q} = M_u u + (M_\alpha + M_{T\alpha}) \alpha + M_{\dot{\alpha}} \dot{\alpha} + M_q q + M_{\delta e} \delta e$$

The introduction of the effect of the gust to these aerodynamic components gives :

$$\dot{u} = -g \cdot \cos \theta_1 \cdot \theta + (X_u + X_{Tu}) u + X_\alpha \alpha + X_\alpha \alpha_g$$

$$+ (X_u + X_{Tu}) u_g + X_{\delta e} \delta e$$

$$\dot{w} = -g \cdot \sin \theta_1 \cdot \theta + Z_u u + Z_\alpha \alpha + Z_{\dot{\alpha}} \dot{\alpha} + (U_1 + Z_q) q +$$

$$Z_u u_g + Z_\alpha \alpha_g + (Z_q - Z_{\dot{\alpha}}) q_g + Z_{\delta e} \delta e$$

$$\dot{q} = M_u u + (M_\alpha + M_{T\alpha}) \alpha + M_{\dot{\alpha}} \dot{\alpha} + M_q q + M_u u_g + (M_\alpha + M_{T\alpha}) \alpha_g + (M_q - M_{\dot{\alpha}}) q_g + M_{\delta e} \delta e$$

The previous equations can be written after applying Laplace transformation in the following form :

$$a_1 \theta(s) + a_2 \alpha(s) + (s+a_3) u(s) =$$

$$a_4 W_g(s) + a_5 u_g(s) + a_6 \delta e(s)$$

$$(b_2 s + b_1) \theta(s) + (b_3 s + b_4) \alpha(s) + b_5 u(s) =$$

$$b_6 W_g(s) + b_7 u_g(s) + b_8 q_g(s) + b_9 \delta e(s)$$

$$(s^2 + C_1^2) \theta(s) + (C_3 s + C_2) \alpha(s) + C_4 u(s) =$$

$$C_5 W_g(s) + C_6 u_g(s) + C_8 q_g(s) + C_7 \delta e(s)$$

where:

$$\begin{aligned}
 a_1 &= g \cdot \cos \theta_1 & b_1 &= g \cdot \sin \theta_1 & c_1 &= -M_q \\
 a_2 &= -X_{\alpha} & b_2 &= -(U_1 + Z_q) & c_2 &= -M_{\alpha} + M_{T\alpha} \\
 a_3 &= -(X_u + X_{Tu}) & b_3 &= U_1 - Z_{\dot{\alpha}} & c_3 &= -M_{\dot{\alpha}} \\
 a_4 &= X_{\alpha}/U_1 & b_4 &= -Z_{\alpha} & c_4 &= -M_u \\
 a_5 &= X_u + X_{Tu} & b_5 &= -Z_u & c_5 &= -M_{\alpha} + M_{T\alpha} \\
 a_6 &= X_{\delta c} & b_6 &= -Z_{\alpha}/U_1 & c_6 &= M_u \\
 & & b_7 &= Z_u & c_7 &= M_{\delta c} \\
 & & b_8 &= Z_q - Z_{\dot{\alpha}} & c_8 &= M_{\delta c} \\
 & & b_9 &= Z_{\delta c} & & 
 \end{aligned}$$

The law for controlling the used auto pilot has the following form for the elevator channel:

$$\Delta \delta c = -i_{\theta} (\theta_s - \theta) + i_{\dot{\theta}} + i_h \Delta h$$

For stabilized level flight conditions ( $\theta_s=0, \Delta h=0$ ), the airplane longitudinal dynamic equations are:

$$\begin{aligned}
 (a_9 - a_8 s) \theta(s) + a_2 \alpha(s) + (s + \alpha_3) u(s) = \\
 a_4 W_g(s) + a_5 u_g(s)
 \end{aligned}$$

$$\begin{aligned}
 (b_{12} + b_{13} s) \theta(s) + (b_3 s + b_4) \alpha(s) + b_5 u(s) = \\
 b_6 W_g(s) + b_7 u_g(s) + b_8 q_g
 \end{aligned}$$

$$\begin{aligned}
 (C_9 + C_{10} s + s^2) \theta(s) + (C_3 s + C_2) \alpha(s) + C_4 u(s) = \\
 C_5 W_g(s) + C_6 u_g(s) + C_8 q_g
 \end{aligned}$$

where:

$$\begin{aligned}
 a_7 &= a_6 \cdot i_{\theta} & b_{10} &= b_9 \cdot i_{\theta} & c_9 &= -c_7 \cdot i_{\theta} \\
 a_8 &= a_6 \cdot i_{\dot{\alpha}} & b_{11} &= b_9 \cdot i_{\dot{\alpha}} & c_{10} &= c_1 - c_7 \cdot i_{\dot{\alpha}} \\
 a_9 &= a_1 - a_7 & b_{12} &= b_1 - b_{10} \\
 & & b_{13} &= b_2 - b_{11}
 \end{aligned}$$

The response of a linear system to a stationary random input can be investigated by the methods employing the spectral densities. The spectral density  $\Phi_Y(\omega)$  of the output magnitude of a linear system with frequency characteristics  $G_{YX}(j\omega)$  is determined by the expression:

$$\Phi_Y(\omega) = |G_{YX}(j\omega)|^2 \Phi_X(\omega) = \Phi_{YX}^2(\omega) \Phi_X(\omega)$$

The mathematical models of the air turbulence are based on statistical methods [2-7]. Using Dryden method, wind velocity components are represented in spectral density distribution. The power spectral densities of these components take the form:

$$\Phi_{u_s}(\Omega) = \sigma_u^2 \frac{2L_u}{\pi(1 + (L_u \Omega)^2)}$$

$$\Phi_{u_f}(\Omega) = \sigma_w^2 \frac{L_w(1 + 3(L_w \Omega)^2)}{\pi[1 + (L_w \Omega)^2]^2}$$

$$\Phi_{q_s}(\Omega) = \Phi_{w_s}(\Omega) \frac{\Omega_2}{\left[1 + \left(\frac{4b\Omega}{\pi^2}\right)^2\right]}$$

The spectral density of the wind is a rational fractional function of the frequency  $\omega$ , in which  $\omega$  is contained in even powers only. The spectral density of the input magnitude, therefore, is represented in the form of the modulus of the frequency characteristics of a linear system (shaping filter).

$$\Phi_X = |G_{XX_1}(j\omega)|^2 = G_{XX_1}^2(\omega)$$

where  $x_1$  is the sinusoidal signal of frequency  $\omega$  supplied to the input to the shaping filter. Consequently, the spectrum distribution of the wind velocity components are obtained in the form:

$$\Phi_{w_g}(j\omega) = \frac{p_1 + jp_2 \omega}{(1 - r^2 \omega^2) + j2r\omega}$$

$$\Phi_{q_g}(j\omega) = \frac{p_3 \omega^2 + jp_4 \omega}{[(1 - r^2 \omega^2) + p_5 \omega^2] + j[(\omega - r^2 \omega^3)p_6 + 2r\omega]}$$

$$\Phi_{u_g}(j\omega) = \frac{p_7}{1 + jr_1 \omega}$$

where

$$\begin{aligned}
 r &= L_w/U_1 & p_1 &= \sigma_w \sqrt{r/\pi} & p_2 &= rp_1 \\
 p_3 &= p_2/U_1 & p_4 &= p_1/U_1 & p_5 &= 8br/\pi U_1 \\
 p_6 &= -4b/\pi U_1 & r_1 &= 2 L_u/\omega & p_7 &= \sigma_u \sqrt{2L_u/\pi U_1}
 \end{aligned}$$

Accordingly the spectral density of the output magnitude yields:

$$\phi_Y(\omega) = |G_{XX1}(j\omega)G_{XY}(j\omega)|^2$$

Then the effects of wind velocity components  $u_g$ ,  $w_g$ , and  $q_g$  upon  $\alpha$ ,  $\theta$ , and  $u$  are obtained by determining the spectrum magnitude of the output for each case. For example, the output spectrum magnitude of the angle of attack due to the vertical wind component is given by:

$$\begin{aligned} \phi_{\alpha w_g}(\omega) &= |G_{\alpha w_g}(j\omega) \cdot G_{w_g}(j\omega)| \\ &= \frac{[(a_{24} - a_{22}\omega^2) + j(a_{23}\omega - a_{21}\omega^3)]}{[(b_{25} + b_{21}\omega^4 - b_{23}\omega^2) + j(b_{24}\omega - b_{22}\omega^3)]} \cdot \frac{P_1 + jP_2(\omega)}{(1 - r^2\omega^2) + j(2r\omega)} \\ &= \left| \frac{AA + jAAA}{BB\omega + jBBB\omega} \right|^2 = \frac{AA^2 + AAA^2}{BB\omega^2 + BBB\omega^2} \end{aligned}$$

and the normalized spectrum magnitude is given by the following relation :

$$\Psi_{\alpha w_g}(\omega) = \frac{\phi_{\alpha w_g}}{\sigma_{w_g}^2}$$

$$\sigma_{w_g}^2 = \int_0^{\infty} \phi_{w_g}(\omega) \cdot d\omega$$

The system is also solved in the time domain by using a digital analysis technique to solve the differential equations of motion. These equations are represented by the block diagram shown in Figure (1), and for  $u_g$  and  $w_g$  either as step input or functional input.

### ANALYSIS AND DISCUSSION

The RPV stability derivatives are computed for several conditions including different flight speeds, flight altitudes, c.g. positions, tail volume ratios, and for two design configurations of horizontal tail.

A program was dedicated to compute the output magnitude of spectral function corresponding to its

frequency. The program was used to calculate the RPV frequency response for the above mentioned conditions, in addition to the case where the RPV is equipped with an auto pilot (altitude corrector) and for both wind conditions (CAT and TST). The response of the RPV ( $\Delta\theta$  and  $\Delta\alpha$ ) caused by the gust components  $u_g$ ,  $w_g$ , and  $q_g$  are given in Figures (2-5). The effect of  $u_g$  and  $q_g$  is evidently very small compared to the effect of  $w_g$ . This is the basis in what follows for analyzing the behavior of the RPV subjected to vertical gust component  $w_g$  only.

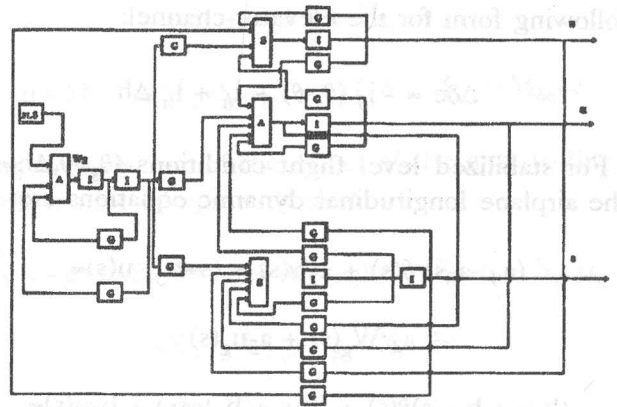


Figure 1. A/C Block diagram for gust input  $W_g$

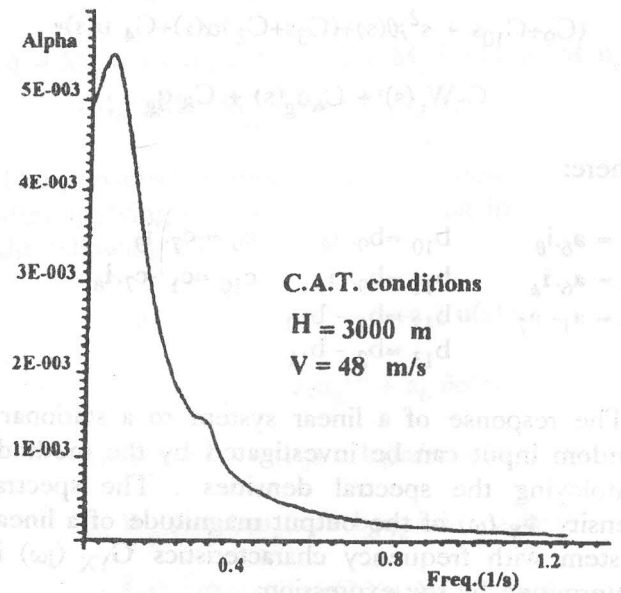


Figure 2. Output spectrum (angle of attack due to vertical gust).



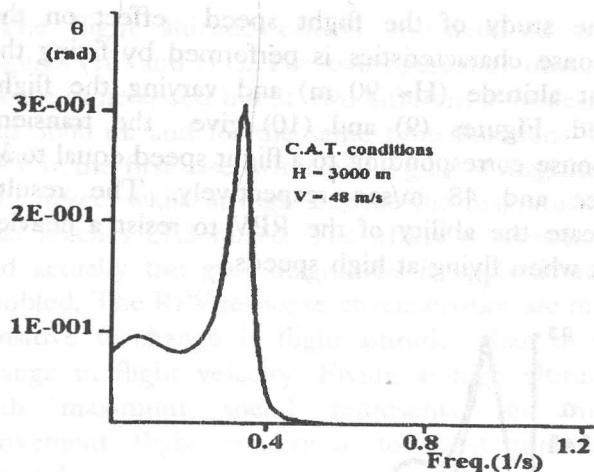


Figure 3. Output spectrum (pitch angle due to vertical gust).

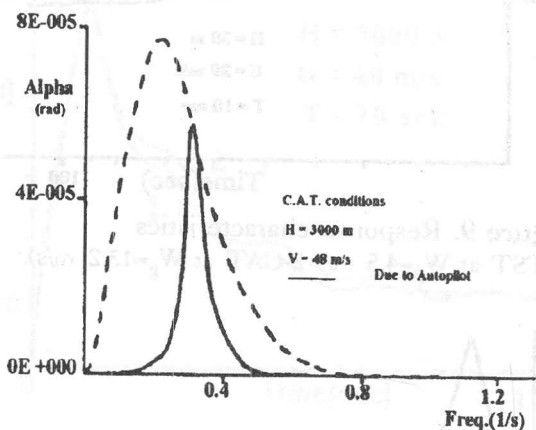


Figure 4. Output spectrum (angle of attack due to horizontal gust).

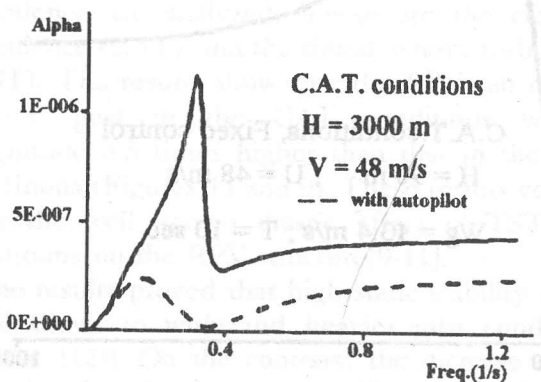


Figure 5. Output spectrum (angle of attack due to pitch rate).

For the analysis in the time domain, the random character of air turbulence could be considered only by introducing the input wind magnitude in the form of a function input. The results given in Figures (6) and (7) illustrate the response characteristics of the RPV subjected to unit step and function inputs. The comparison shows that a function-input response could be replaced by a unit step-input response (with average value of wind magnitude) without essential changes in the response characteristics.

At very low frequencies, Figures (2) and (3) indicate the existence of peaks of considerable amplitude in the angle of attack and the pitch angle response characteristics. This is well confirmed by the results obtained in time domain response, of the RPV subjected to vertical air flow with different magnitudes and for different time duration, fig. 8. These response characteristics obtained matches well with the results obtained by Moubolt [8].

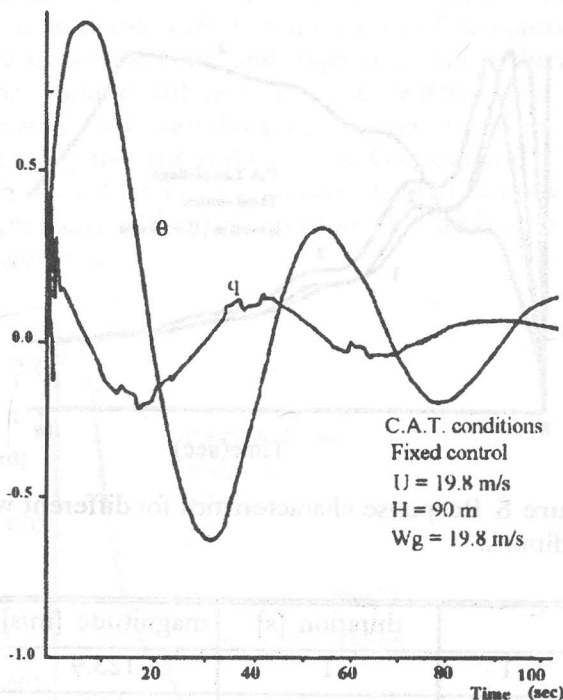


Figure 6. Response characteristics (function input).

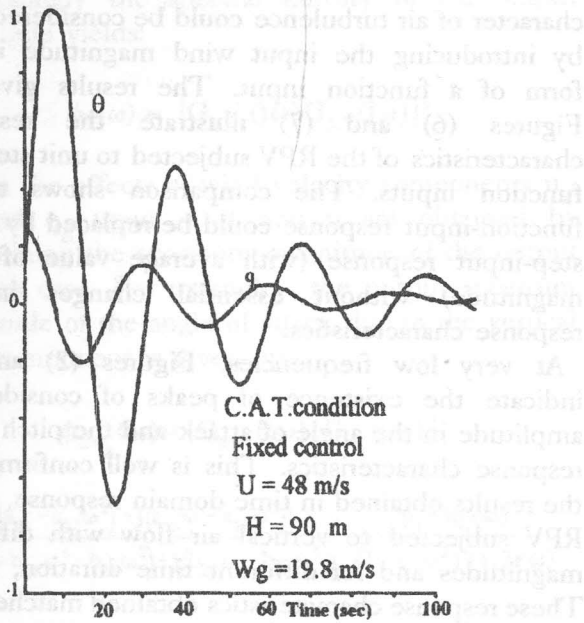


Figure 7. Response characteristics (step input).

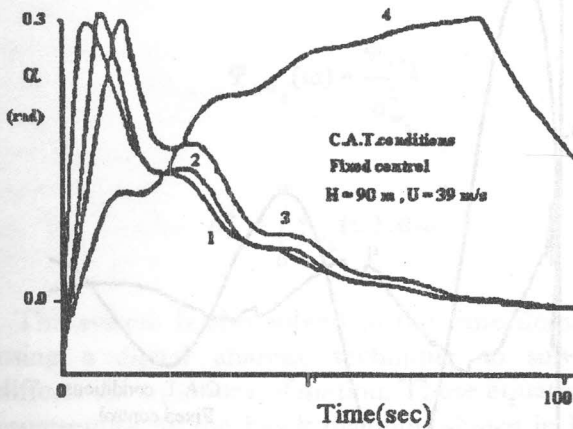


Figure 8. Response characteristics for different wind conditions.

	duration [s]	magnitude [m/s]
1	1	123.9
2	5	24.9
3	10	13.8
4	30	4.95

The study of the flight speed effect on the response characteristics is performed by fixing the flight altitude ( $H=90$  m) and varying the flight speed. Figures (9) and (10) give the transient response corresponding to a flight speed equal to 39 m/sec and 48 m/sec respectively. The results indicate the ability of the RPV to resist a heavier gust when flying at high speeds.

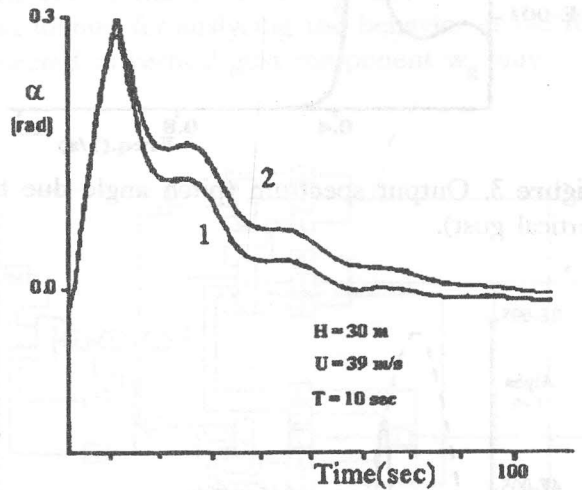


Figure 9. Response characteristics (1-TST at  $W_g=4.5$  m/s 2-CAT at  $W_g=13.2$  m/s).

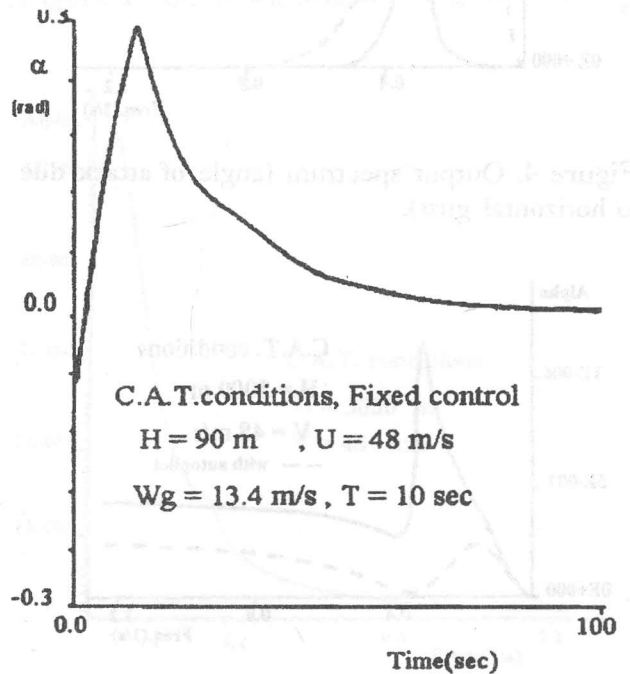


Figure 10. Response characteristics (CAT; fixed condition)

The flight altitude effects are deduced from Figures (10) and (11). The two figures are obtained for the same speed but at two different altitudes, 90 and 3000 m. and for the same time duration. The RPV in the first case, withstood a gust of magnitude 14.7 m/sec, while at high altitude the magnitude of gust reaches 27.3 m/sec. The effect is remarkable and actually the gust magnitude is approximately doubled. The RPV response characteristics are more sensitive to change in flight altitude than to the change in flight velocity. Flying at high altitudes with maximum speed represents the most convenient flight conditions to resist turbulent atmosphere.

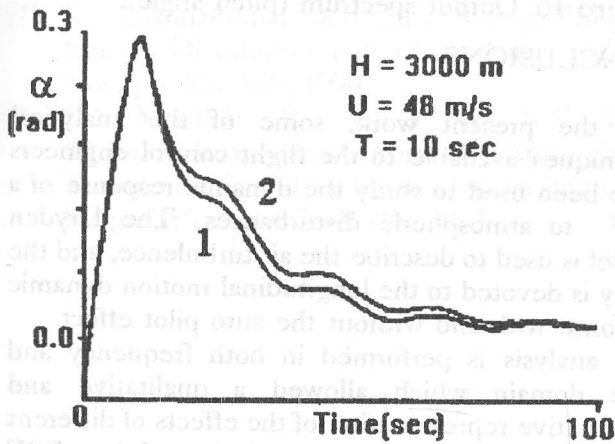


Figure 11. Response characteristics (1-TST at  $W_g=7.2$  m/s 2- CAT at  $W_g=27.3$  m/s).

In the present study, the effect of two types of turbulence are analyzed. These are the clear air turbulence (CAT), and the thunderstorm turbulence (TST). The results show that the RPV can resist a vertical gust in the CAT conditions with a magnitude 3.5 times higher than that in the TST conditions (Figures 11 and 9). These results confirm with the well known drastic effect of TST gust conditions on the RPV structure[9-11].

The results proved that high static stability of the RPV allows to withstand heavier gust conditions (Figure (12)). On the contrary, the increase of the gust duration decreases the ability of the RPV to withstand vertical gust (Figure 8).

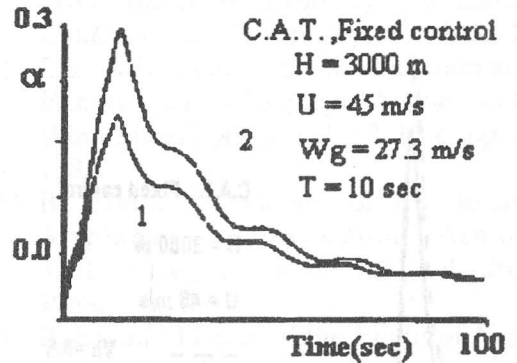


Figure 12. Response characteristics (1- High static stability 2- low static stability).

The change of the horizontal tail volume ratio has a noticeable effect on the aircraft stability derivatives. The reduction of this value results in a remarkable improvement of the response characteristics in the case of fixed control. The peaks formed at low frequency, are less pronounced. However, for free control (with auto pilot), the response characteristics are deteriorated and the peaks are augmented (Figures (13), (14) and (15)). This undesirable effect in the case of free control is easily understandable and expected. The reduction in the volume tail ratio is done, when fixing the horizontal tail aerodynamic center position, by decreasing the tail surface area. Consequently, the auto pilot efficiency is reduced. A good remedy for this problem, is the use of all-movable horizontal tail arrangement.

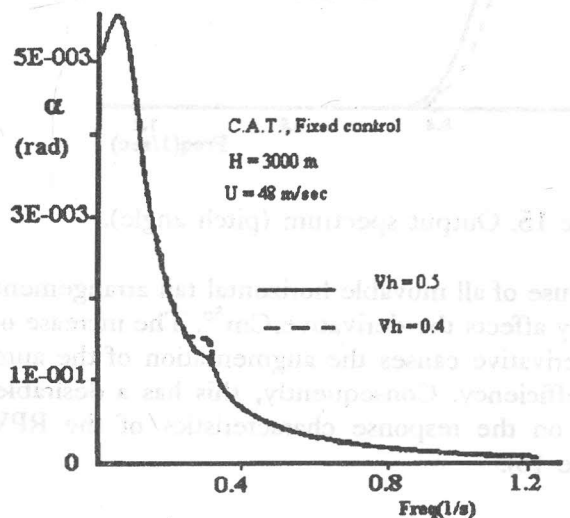


Figure 13. Output spectrum (angle of attack).

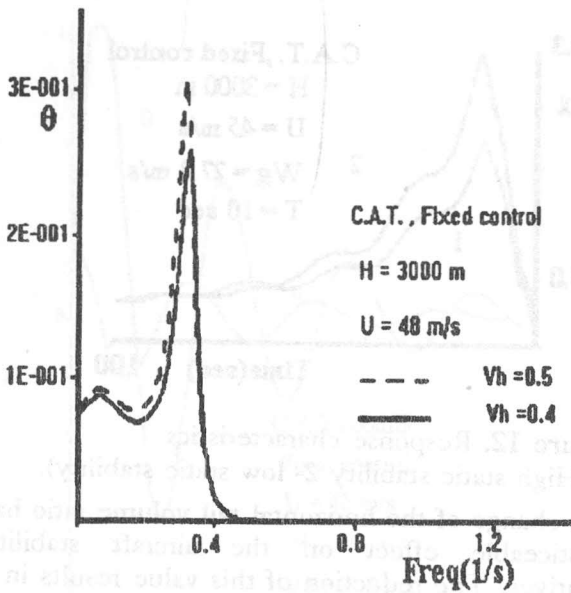


Figure 14. Output spectrum (pitch angle).

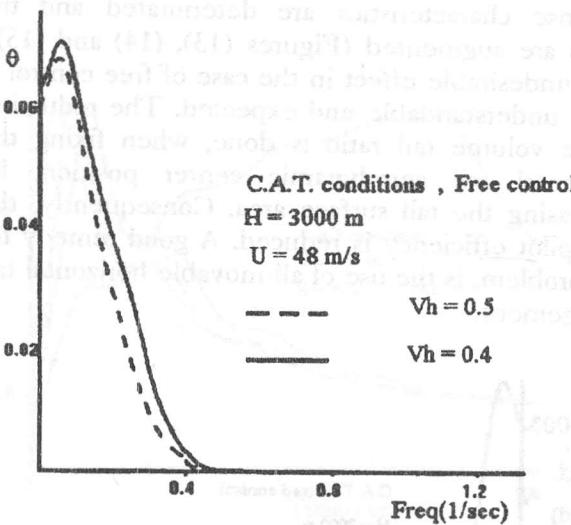


Figure 15. Output spectrum (pitch angle).

The use of all movable horizontal tail arrangement actually affects the derivative  $Cm^{\delta c}$ . The increase of this derivative causes the augmentation of the auto pilot efficiency. Consequently, this has a desirable effect on the response characteristics of the RPV (Figure 16).

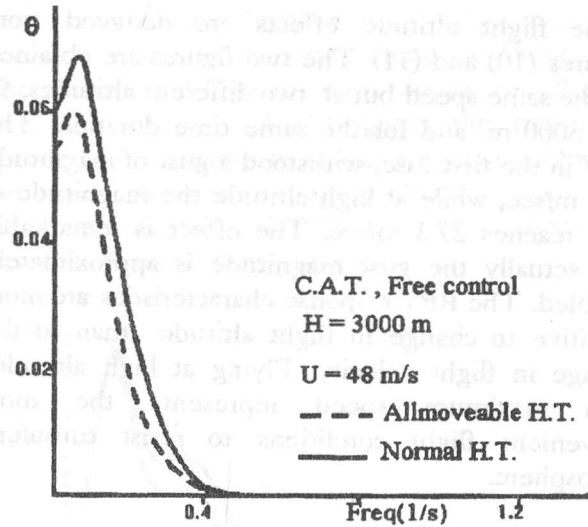


Figure 16. Output spectrum (pitch angle).

CONCLUSIONS

In the present work, some of the analytical techniques available to the flight control engineer have been used to study the dynamic response of RPV to atmospheric disturbances. The Dryden model is used to describe the air turbulence, and the study is devoted to the longitudinal motion dynamic response with and without the auto pilot effect. The analysis is performed in both frequency and time domain which allowed a qualitative and quantitative representation of the effects of different parameters. A satisfactory description of the RPV response to random wind input have been achieved by a step input response in the time domain. The results obtained agreed well with earlier investigations and proved the effectiveness of the method.

The importance of the high altitude effect has been demonstrated. The resistibility of the RPV to the turbulent air conditions increases with the increase of altitude. The influence in the response characteristics is strong enough to cancel the effects of other less-dominant parameters such as the flight velocity.

Both the flight speed and the static stability allowed a favorable effect on the dynamic behavior of the RPV in turbulent air. The analysis proved the necessity of using the auto pilot (altitude corrector) to resist the turbulence effects. In all cases, it was found that (TST) conditions are not recommended for safe flight.



## REFERENCES

- [1] Jan Roskam, "Airplane Flight Dynamics and Automatic Flight Control", *Roskam Aviation and Engineering Corporation*, 1982.
- [2] J.L. Doob, *Stochastic Processes*, John Wiley and Sons, Inc., 1976.
- [3] Gourik Bhattacharyya and Richard A. Johnson, *Statistical Concepts and Methods*, John Wiley and Sons, Inc., 1973.
- [4] Yu. P. Dobrolenskiy, "Flight Dynamics in Moving Air", *NASA TT F-600*, 1969.
- [5] Bernard Etkin, *Dynamics of Atmospheric Flight*, John Wiley and Sons Inc., 1971.
- [6] C. Robert. Nelson, *Flight Statistics and Automatic Control*, McGraw-Hill Book Company, 1989.
- [7] K. Krishnakumar and J.E. Bailey, "Inertial Energy Distribution", *J. of Guidance*. vol. 13, Nov. pp. 557-559, 1990.
- [8] J.C. Moubolt, R. Steiner and K.G. Prat, "Dynamic Response of Airplanes to Atmospheric Turbulence Including Flight Data on Input and Response", *NASA TR-R-199*, 1964.
- [9] Vladimir Bochis, "Dynamics of an Aircraft in Wind Shear of Arbitrary Direction". *J. of Guidance*, vol. 7, Sept. pp. 339-343., 1984.
- [10] J.E. Baily and K.S. Krishnakumar, "Total Energy Control Concepts Applied to Flight in Wind Shear", *AIAA*, vol. 12, Dec. pp. 344-347, 1982.
- [11] B. Etkin. "A Theory of the Response of Airplanes to Random Atmospheric Turbulence", *J. Aero. Sci.*, vol. 26, No. 7, 1959.
- [12] B. Etkin, "Theory of the Flight of Airplanes in Isotropic Turbulence - Review and Extension", *AGARD Rep. 372*, 1961.
- [13] G.B. Skelton, "Investigation of the Effects of Gusts on V/STOL Craft in Transition and Hover", *USAF Rep. AFFDL-TR-68-85*, 1968.
- [14] H.S. Ribner, "Spectral Theory of Buffeting and Gust Response - Unification and Extension", *J. Aero. Sci.*, vol. 23, No. 12, 1956.
- [15] J.B. Barlow, "Theory of Propeller Forces in a Turbulent Atmosphere", *Univ. of Toronto UTIAS Rep. 155*, 1970.
- [16] Donald McLean, "Automatic Flight Control Systems", *Hall International*, (U.K.) Ltd., 1990.